

Supplementary Information for

On the inconsistencies of metalens performance reports

Rajesh Menon^{1,2,*} & Berardi Sensale-Rodriguez

¹Department of Electrical & Computer Engineering, University of Utah, 50 Central Campus Dr., Salt Lake City, UT 84112, USA.

²Oblate Optics, Inc., San Diego, CA 92130, USA

*rmenon@eng.utah.edu

1. Diffraction orders:

When a diffraction grating is illuminated by a plane wave, the transmitted field is often expressed as a linear combination of plane waves, referred to as diffraction orders. The ratio of the power carried away by each plane wave to the total incident power is referred to as the diffraction efficiency. Although less well known, this analysis can be applied to diffractive lenses as well [1]. As illustrated below, the transmitted field can be easily decomposed into a linear combination of spherical waves (converging and diverging), which form a complete basis set. In the case of diffractive lenses, the diffraction efficiency is similarly defined as the ratio of power carried by one of these spherical waves to the total incident power. The convention of notation for these orders is illustrated in Fig. 1(a).

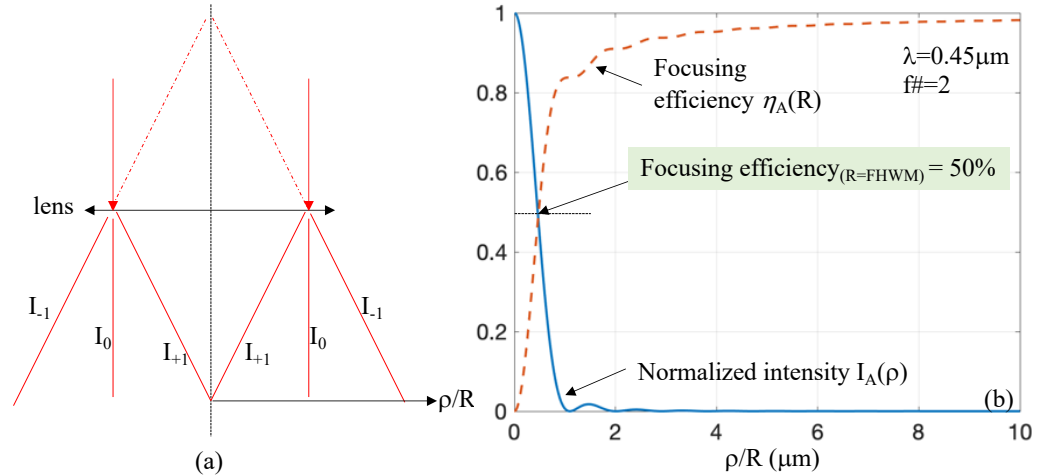


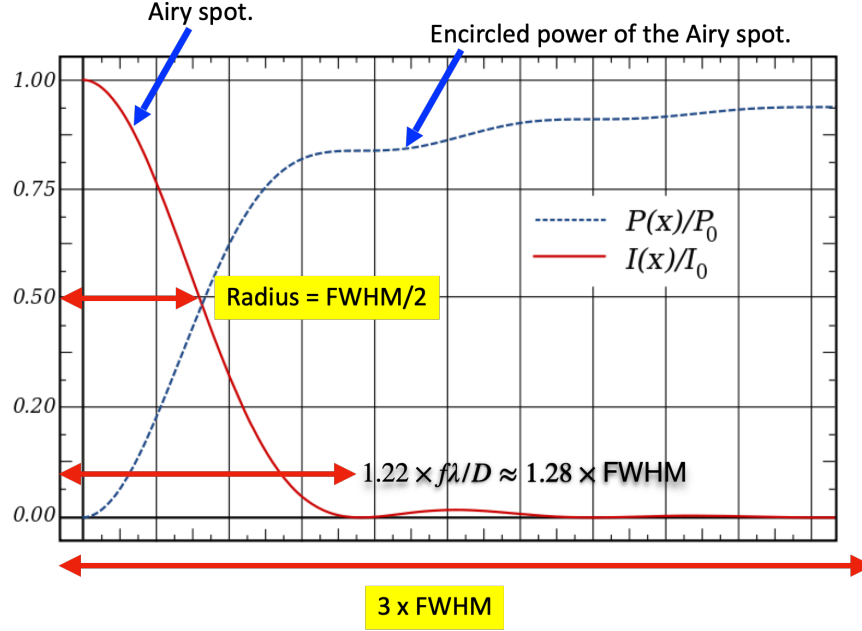
Figure S1: (a) Diffraction orders of a lens are the spherical wave decomposition of the transmitted field. (b) Airy function is the PSF of a lens with 100% diffraction efficiency into the 1st order. Focusing efficiency is defined as the ratio of power inside a spot of radius R in the focal plane to the incident power. This is also referred to as the encircled power. In the case of an ideal lens (Airy function), it is equal to 50% when the radius R is equal to the full-width at half-maximum of the PSF.

Consequently, the point-spread function (PSF), which is the intensity distribution in the focal plane of a lens when the lens is illuminated by a plane wave can be expressed as: $I(\rho) = I_0 + I_{+1}(\rho) + I_{-1}(\rho) + \dots$, where I_0 is the spatially uniform 0th diffracted order, the subscript refers to the order of diffraction, the sign in the subscript refers to whether the spherical wave is

converging (+) or diverging (-), and the sum occurs for all propagating diffracted orders. Note that we assumed the simple case of cylindrical symmetry (and normal incidence or on-axis focusing) for simplicity, but the principle applies generally.

The encircled power is defined as $E(R) = \int_0^R I(\rho) \rho d\rho$, where R is the radius of the spot over which the power is encircled. If one ignores Fresnel reflection losses at the interfaces and absorption losses in the material, then $E(R = \infty) = E_0$, the total incident power. Then, the focusing efficiency is given simply by $\eta(R) = \frac{E(R)}{E_0}$. As expected, the focusing efficiency is dependent upon the size of the focal spot, R . In the case of polarization sensitive lenses, it is important to ensure that E_0 accounts for incident power with unpolarized light (if this metric is used to compare to conventional polarization insensitive lenses).

Next, one may ask the question what is the focusing efficiency of an ideal lens. Diffraction ensures that a lens cannot have 100% focusing efficiency, even when the diffraction efficiency of one order may be 100%. To illustrate this point, we can consider an ideal lens with 100% diffraction efficiency into its 1st order. The PSF of such a lens is simply the Airy function, $I_A(\rho) = I_{A0} \left(\frac{2J_1(x)}{x} \right)^2$, where I_{A0} is the incident intensity, $J_1(x)$ is the Bessel function of the 1st kind, and $x = \frac{\pi \rho}{\lambda f\#}$, where λ is the wavelength and $f\#$ is the f number of the lens. The encircled power of the Airy function can be analytically expressed as: $E_A(R) = \int_0^R I_A(\rho) \rho d\rho = E_{A0} \left(1 - J_0^2\left(\frac{\pi R}{\lambda f\#}\right) - J_1^2\left(\frac{\pi R}{\lambda f\#}\right) \right)$, where E_{A0} is the total incident power. Then, the focusing efficiency is simply given by: $\eta_A(R) = \left(1 - J_0^2\left(\frac{\pi R}{\lambda f\#}\right) - J_1^2\left(\frac{\pi R}{\lambda f\#}\right) \right)$. From this expression, we can readily show that the focusing efficiency when R = full-width at half-maximum (FWHM) of the PSF is 50% (see Fig. S2b). In other words, a lens with 100% diffraction efficiency can have focusing efficiency of 50% (measured with R =FWHM). We further emphasize that reporting focusing efficiency without reporting the size of the focused spot is incomplete. Complete information about focusing efficiency requires the encircled power.



Radius used for focusing efficiency measurements.

Figure S2: Airy spot and its encircled power.

Table S1: Summary of reported metalens efficiencies (only one example from each reference is shown for brevity). The bound from ref [2] is computed based on the unit-cell period and NA from Fig. 2a in [2]. All values in this table are for monochromatic lenses. Those values marked in red exceed bounds dictated by the unit-cell design method [2]. {*focal spot size = 5 X FWHM. **focal spot size = 4 X FWHM.}

Reference	λ	NA	Unit-cell period (Δ/λ)	Radius of focal spot (FWHM)	Reported eff.	Bound from Ref [2]
[4]	405nm	0.8	0.49	Not disclosed	88%	64.6%*
[6]	660nm	0.85	0.53	2 sim, 4 expt.	84% sim, 60% expt.	56.5%**
[7]	532nm	0.9	0.45	Not disclosed	42%	58.5%*
[8]	532nm	0.98	0.41	3	67%	45%
[9]	405nm	0.8	0.49	Not disclosed	86%	64.6%*
[10]	915nm	0.95	Grating averaging	10	77%	-
[11]	1,550nm	0.89	0.52	3	72%	51.9%

Notes on efficiency reports:

In Ref [4], the supplement includes this statement:

“For efficiency measurements, we used a supercontinuum laser (SuperK) as the source. The efficiency is defined as the ratio of the optical power of the focused beam to the optical power of the incident beam, as captured by a photodetector (Thorlabs S120C) located at the same

position as the CMOS camera. The incident optical power was measured as the light passing through an aperture (aluminum on glass) with the same size as the metalens.”

Based on this text and the Fig. S2 in the supplement of ref [4], we surmise that an aperture (or iris) was likely not used to measure the focused power. Therefore, this reported efficiency may include both the desired and undesired diffracted orders.

In Ref. [5], Fig. S3 in the supplement indicates that there is no aperture in the focal plane when measuring the focused power. Therefore, we speculate that the reported efficiency might have the same issue as in Ref. [4].

Ref [6] states:

“The efficiency is calculated as the ratio of the optical power of the measured focused beam to that of the incident beam. The incident beam was measured as the optical power passing through a circular aperture (aluminum on glass) with the same diameter (300 μm) as the metalenses.”

Later with regard to Fig 4, it states:

“We define the efficiency as the ratio of the optical power in the focal spot area (circle of radius $2 \times \text{FWM}$ spanning the center of the focal spot) to the incident optical power.”

We further note that the experimental efficiencies are from results in Fig. S3b, while simulations are shown in Fig. 4. In the caption of Fig. S2b (regarding measurement of focusing efficiencies), it states:

“The diameter of the iris was about eight times of the FWHMs of the focal spots of the metalenses (at design wavelength) on the image plane of the set-up.”

So, the radius of focal spot is different for simulation and experiment. We computed the bound for the larger radius (4 x FWHM) to be conservative.

In Ref [7], the main text states:

“The focusing efficiency is defined as the power of focal spot divided by incident light in the case of circularly polarized light.”

and the caption of Fig. S3 says:

“The efficiency was measured, in case of circularly polarized incidence, by dividing the power of the focal spot by the total power passing through an aperture with the same diameter as the water immersion meta-lens.”

Otherwise, no information is provided regarding the radius of the focal spot used for measuring efficiencies. We used a radius of 5 X FWHM to compute the bound.

Ref [8] states:

“the focusing efficiency can be defined as the fraction of the incident light that passes through a circular iris in the focal plane with a radius equal to three times the fwhm spot size, so defined as the total power in the desired focal spot divided by the total incident power.”

Ref [9] states:

“For efficiency measurements, a tunable laser (SuperK, NTK Photonics) was used and the CMOS camera was replaced by a photodetector (Thorlabs S120C). The efficiency is defined as the ratio of the optical power of the focused beam to the optical power of the incident beam. The latter was measured as the optical power passing through a circular aperture (aluminum on glass) with the same diameter as the metalenses.”

There is no other information about the radius of the focal spot.

Ref [10] says:

“The focusing efficiency is defined as the percentage of the power incident on the metalens aperture that is focused into and passes through a circle with a radius of 5 μm centered around

the focal spot of the metalens. The radius of $5\text{ }\mu\text{m}$ for the aperture is selected for a direct comparison with the experimentally measured results that are presented in the next section.”

For the experiments, it says:

“We measured the focusing efficiency of the metalens using the setup shown in Fig. 4f”

“The intensity distribution at the metalens focal plane was magnified by $100\times$, masked by passing through a 1-mm-diameter aperture in the image plane (corresponding to a $5\text{-}\mu\text{m}$ -radius aperture in the metalens focal plane), and its power was measured. To measure the incident optical power, we focused the incident beam using a commercial lens (Thorlabs AC254- 030-B-ML with a focal length of 3 cm and a transmission efficiency of 98%) and measured its power in the image plane (Fig. 4g). The focusing efficiency of the metalens was found as 77% by dividing the power passed through the aperture in Fig. 4f to the incident power.”

From Fig. 4(d), we can estimate the FWHM as $0.5\mu\text{m}$, which gives a spot radius of $10\times$ FWHM.

Ref [11] says:

“we define the focusing efficiency as the fraction of the incident light that passes through a circular aperture in the plane of focus with a radius equal to three times the FWHM spot size.”

Supplement References:

- [1] D. Attwood, *Soft X-rays and Extreme Ultraviolet Radiation: Principles and Applications* (Cambridge University Press, 1999).
- [2] Haejun Chung and Owen D. Miller, "High-NA achromatic metalenses by inverse design," *Opt. Express* **28**, 6945-6965 (2020).
- [3] D. W. Prather, D. Pustai, and S. Shi, "Performance of multilevel diffractive lenses as a function of f-number," *Appl. Opt.* **40**, 207–210 (2001).
- [4] M. Khorasaninejad, W. T. Chen, R. C. Devlin, J. Oh, A. Y. Zhu, and F. Capasso, "Metalenses at visible wavelengths: Diffraction-limited focusing and subwavelength resolution imaging," *Science* **352**, 1190–1194 (2016).
- [5] J. Engelberg, C. Zhou, N. Mazurski, J. Bar-David, A. Kristensen, and U. Levy, "Near-ir wide-field-of-view huygens metalens for outdoor imaging applications," *Nanophotonics* **9**, 361–370 (2020).
- [6] M. Khorasaninejad, A. Y. Zhu, C. Roques-Carnes, W. T. Chen, J. Oh, I. Mishra, R. C. Devlin, and F. Capasso, "Polarization-insensitive metalenses at visible wavelengths," *Nano Lett.* **16**, 7229–7234 (2016). PMID: 27791380.
- [7] Wei Ting Chen, Alexander Y. Zhu, Mohammadreza Khorasaninejad, Zhujun Shi, Vyshakh Sanjeev, and Federico Capasso, "Immersion Meta-Lenses at Visible Wavelengths for Nanoscale Imaging," *Nano Letters* **2017** *17* (5), 3188-3194.
- [8] Haowen Liang, Qiaoling Lin, Xiangsheng Xie, Qian Sun, Yin Wang, Lidan Zhou, Lin Liu, Xiangyang Yu, Jianying Zhou, Thomas F Krauss, and Juntao Li, "Ultrahigh Numerical Aperture Metalens at Visible Wavelengths" *Nano Letters* **2018** *18* (7), 4460-4466.
- [9] M. Khorasaninejad *et al.*, "Visible Wavelength Planar Metalenses Based on Titanium Dioxide," in *IEEE Journal of Selected Topics in Quantum Electronics*, vol. 23, no. 3, pp. 43-58, May-June 2017, Art no. 4700216, doi: 10.1109/JSTQE.2016.2616447.
- [10] Arbabi, A., Arbabi, E., Mansouree, M. *et al.* Increasing efficiency of high numerical aperture metasurfaces using the grating averaging technique. *Sci Rep* **10**, 7124 (2020).
- [11] Arbabi, A., Horie, Y., Ball, A. *et al.* Subwavelength-thick lenses with high numerical apertures and large efficiency based on high-contrast transmitarrays. *Nat Commun* **6**, 7069 (2015).

Version of comment with complete list of references:

.

On the inconsistencies of metalens performance reports

Rajesh Menon^{1,2,*} and Berardi Sensale-Rodriguez¹

¹Department of Electrical & Computer Engineering, University of Utah, 50 Central Campus Dr. Salt Lake City UT 84112

²Oblate Optics, Inc. San Diego CA 92130

*rmenon@eng.utah.edu

ABSTRACT

We posit that inconsistent interpretations of experimental data have led to inaccurate claims on metalens focusing efficiencies. By performing a meta-analysis, we show that extraordinary claims of high focusing efficiency at high numerical apertures are, unfortunately, not yet backed by rigorous simulation or experimental results.

The amplitude zone plate, the phase zone plate and the blazed zone plate as well as generalizations of these via multi-level and effective-medium implementations, including those containing sub-wavelength features have historically been considered under the umbrella of diffractive lenses.¹ Recently, flat imaging/focusing elements that contain sub-wavelength features have been rebranded as metalenses.² First, we note that such a definition includes phase Fresnel zone plates with numerical aperture (NA) > 0.5 (note that smallest zone width $= \lambda / (2 \times \text{NA})$) and their high-NA cousins like photon sieves,³ superoscillating flat lenses,^{4,5} super-lenses,⁶ transformation-optics-based lenses,^{7,8} radially-polarized focusing lens,⁹ photonics-crystal-based lenses,¹⁰ and many others. We also note that sub-wavelength features have been applied in diffractive lenses directly to map the required phase transformation,¹¹ using effective-medium theory (and sub-wavelength dielectric pillars),^{12,13} and also with optimization-based inverse design^{14,15} well before the rebranding occurred. Since the definition of a metalens is all-encompassing, it seems a bit absurd to discuss its difference from a diffractive lens. Nevertheless, most articles on metalenses claim two major advantages over diffractive lenses.^{2,16} First, it is suggested that they achieve focusing efficiencies that are higher than those of diffractive lenses at high numerical aperture (NA). Secondly, it is claimed that metalenses achieve multi-functional performance, with the implication that diffractive lenses do not. Hence, our purpose in writing this comment is to motivate and encourage the community to systematically establish these benefits. It is instructive that the focusing efficiency of high-NA multi-level diffractive lenses was calculated using rigorous electromagnetic theory in a seminal paper published in 2001.¹⁷ Even before this work, it was shown that the sharp drop-off in efficiency for high-NA diffractive lenses can be avoided by optimization of the local geometry, both in simulations^{18,19} and in experiments.²⁰ It was shown that even higher efficiencies could be obtained in the context of imaging at high NA.²¹

Next, we note that many prior measurements of focusing efficiencies of metalenses might be erroneous. The focusing efficiency, η is generally defined as the fraction of incident power that is focused to the nominal focal spot. The power in the focal spot is measured by using an iris to restrict the focal region to a **radius** ranging from $3\times$ to $\geq 18\times$ the full-width-at-half-maximum (FWHM) of the focal spot, and sometimes with no iris at all.^{22,23} The incident power is measured effectively by placing the power meter in front of the lens with an iris whose radius equals that of the lens itself. The ratio of these two measurements is reported as focusing efficiency. In the ideal situation, where all light is diffracted into a single focusing order and when $\text{NA} \lesssim 0.8$, the radius of the focal spot is not important as long as it is larger than several times FWHM. This can be seen readily by inspecting the focusing efficiency of the ideal Airy disk (Fig. 1a). However, in a real flat lens, many undesired diffraction orders exist (Fig. 1b), and, if the radius of the focal spot is much larger than the FWHM, the focusing efficiency can be grossly over-estimated, since the desired and undesired diffraction orders become conflated in the efficiency calculation. For example, refs.²⁴ and²⁵ use irises of radius $8.5\times$, $40\times$ FWHM, respectively, while refs.²³ and²² employ no iris. In some cases, focusing efficiencies higher than those theoretically possible (bounded by a unit-cell-based design)²⁶ have also been reported (see Table S1 in ref.²⁷). The unit-cell-based design cannot exactly represent the required phase transformation, leading to extra undesired diffraction orders. Similar issues have also been recently raised and possible solutions proposed.²⁸ But, we note that new solutions are not necessary as this issue of undesired diffraction orders was carefully analyzed some decades ago,²⁹ and it was noted that extreme care must be taken when measuring efficiencies. Finally, as far as we can tell, there has been no direct

experimental comparison between the focusing efficiency of a metalens and an optimized diffractive lens (for instance, similar to ones in ref.²⁰) of the same specification.

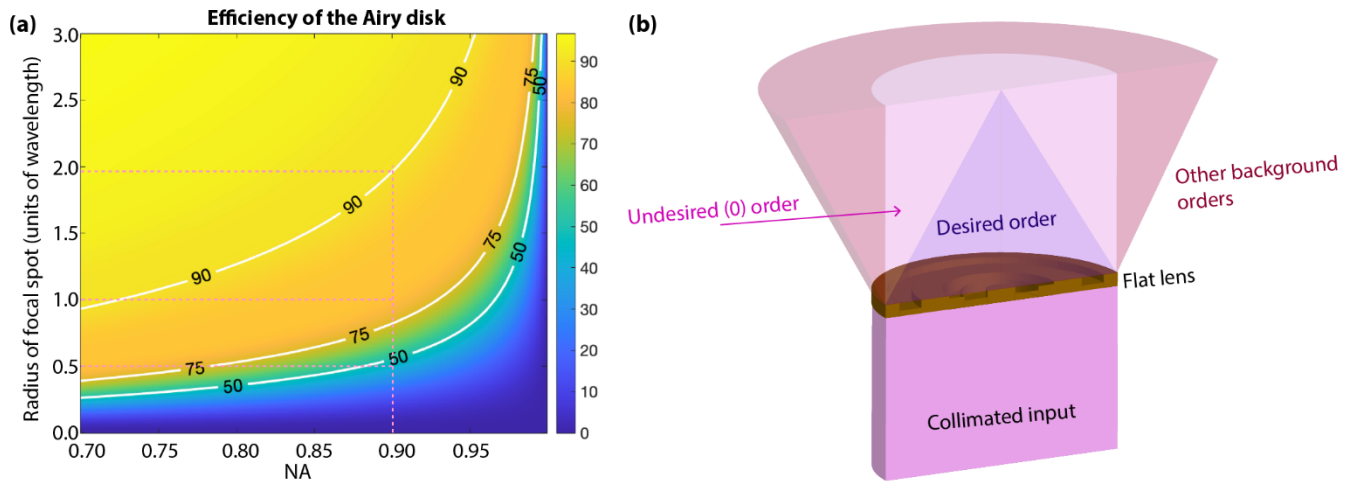


Figure 1. Focusing efficiency of the ideal Airy disk and illustration of diffraction orders from flat lenses. (a) Focusing efficiency, η of the ideal Airy disk as function of NA and the radius of the focal spot, R (normalized to $\text{FWHM}=0.5\lambda/\text{NA}$). For $\text{NA} \lesssim 0.8$, η is stable for $R > 3 \times \text{FWHM}$. But for higher NA, η varies rapidly with R . **(b)** All real flat lenses generate not only the desired diffraction order, but a multitude of undesired orders. Therefore, if $R \gg \text{FWHM}$, then focusing efficiency can be grossly over-estimated.

At this juncture, we also note that there may be over-estimations in the calculations of the Strehl ratio and the modulation-transfer function (MTF). In the case of Strehl ratio, the measured PSF is normalized to the Airy function by matching their encircled powers (area under the curve of the PSF). However, the encircled power is typically only calculated over a very small area, which dramatically overestimates the Strehl ratio. For example, in ref.³⁰, this normalization is performed by integrating the power over a radius of only $3 \times \text{FWHM}$. A related problem is also seen in the calculation of the MTF, which is often calculated as the absolute value of the Fourier transform of the PSF. If the PSF is prematurely truncated (often due to the limited field-of-view of a magnifying objective), the MTF can be grossly overestimated. These errors lead to reports of a high Strehl ratio with modest focusing efficiencies,^{31,32} which is not mathematically possible.

The second advantage of multi-functionality is claimed based on the observation that a metalens "can function differently depending on different degrees of freedom of light (wavelength, polarization, incident angle and so on)," quoting from ref.¹⁶ We note that "conventional" diffractive optics have also demonstrated multi-functionality, *i.e.*, performed different functions based on polarization,^{33,34} wavelength^{35–38} and incident angle.^{39,40}

Our goal in pointing out these discrepancies is to clarify our understanding of the potential of flat lenses. By dramatically increasing the degrees-of-freedom, sub-wavelength diffractive lenses offer a treasure trove of possibilities for imaging and inferencing. By rigorously characterizing their performance, particularly in relation to what has been demonstrated before, we hope that the community can advance their adoption and hopefully enable many exciting applications.

References

1. Mait, J. N. & Prather, D. W. *Selected Papers on Subwavelength Diffractive Optics*, vol. MS 166 of *SPIE Milestone Series* (SPIE Press, 2001).
2. Engelberg, J. & Levy, U. The advantages of metalenses over diffractive lenses. *Nat. communications* **11**, 1991 (2020).
3. Kipp, L. *et al.* Sharper images by focusing soft x-rays with photon sieves. *Nature* **414**, 184–188 (2001).
4. Huang, F. M., Chen, Y., De Abajo, F. J. G. & Zheludev, N. I. Optical super-resolution through super-oscillations. *J. Opt. A: Pure Appl. Opt.* **9**, S285 (2007).
5. Rogers, E. T. *et al.* A super-oscillatory lens optical microscope for subwavelength imaging. *Nat. materials* **11**, 432–435

(2012).

6. Fang, N., Lee, H., Sun, C. & Zhang, X. Sub-diffraction-limited optical imaging with a silver superlens. *Science* **308**, 534–537 (2005).
7. Xu, L. & Chen, H. Conformal transformation optics. *Nat. Photonics* **9**, 15–23 (2015).
8. Roberts, D., Kundtz, N. & Smith, D. Optical lens compression via transformation optics. *Opt. Express* **17**, 16535–16542 (2009).
9. Yu, A.-p. *et al.* Creation of sub-diffraction longitudinally polarized spot by focusing radially polarized light with binary phase lens. *Sci. Reports* **6**, 38859 (2016).
10. Minin, I. V., Minin, O. V., Triandaphilov, Y. R. & Kotlyar, V. V. Subwavelength diffractive photonic crystal lens. *Prog. In Electromagn. Res. B* **7**, 257–264 (2008).
11. Kipfer, P. *et al.* Infrared optical components based on a microrelief structure. *Opt. Eng.* **33**, 79–84 (1994).
12. Chen, F. T. & Craighead, H. G. Diffractive lens fabricated with mostly zeroth-order gratings. *Opt. letters* **21**, 177–179 (1996).
13. Chen, F. & Craighead, H. G. Diffractive phase elements based on two-dimensional artificial dielectrics. *Opt. letters* **20**, 121–123 (1995).
14. Zhou, Z. & Drabik, T. J. Optimized binary, phase-only, diffractive optical element with subwavelength features for 1.55 μm . *JOSA A* **12**, 1104–1112 (1995).
15. Prather, D. W., Mait, J. N., Mirotznik, M. S. & Collins, J. P. Vector-based synthesis of finite aperiodic subwavelength diffractive optical elements. *JOSA A* **15**, 1599–1607 (1998).
16. Arbabi, A. & Faraon, A. Advances in optical metalenses. *Nat. Photon.* **17**, 16–25, DOI: [10.1038/s41566-022-01108-6](https://doi.org/10.1038/s41566-022-01108-6) (2023).
17. Prather, D. W., Pustai, D. & Shi, S. Performance of multilevel diffractive lenses as a function of f-number. *Appl. Opt.* **40**, 207–210, DOI: [10.1364/AO.40.000207](https://doi.org/10.1364/AO.40.000207) (2001).
18. Sheng, Y., Feng, D. & Larochelle, S. Analysis and synthesis of circular diffractive lens with local linear grating model and rigorous coupled-wave theory. *JOSA A* **14**, 1562–1568 (1997).
19. Schmitz, M. & Bryngdahl, O. Rigorous analysis and design of diffractive cylindrical lenses with high numerical and large geometrical apertures. *Opt. communications* **153**, 118–124 (1998).
20. Finlan, J. M., Flood, K. M. & Bojko, R. J. Efficient f/1 binary-optics microlenses in fused silica designed using vector diffraction theory. *Opt. Eng.* **34**, 3560–3564 (1995).
21. Blomstedt, K., Noponen, E. & Turunen, J. Surface-profile optimization of diffractive 1: 1 imaging lenses. *JOSA A* **18**, 521–525 (2001).
22. Engelberg, J. *et al.* Near-ir wide-field-of-view huygens metalens for outdoor imaging applications. *Nanophotonics* **9**, 361–370, DOI: [doi:10.1515/nanoph-2019-0177](https://doi.org/10.1515/nanoph-2019-0177) (2020).
23. Khorasaninejad, M. *et al.* Metalenses at visible wavelengths: Diffraction-limited focusing and subwavelength resolution imaging. *Science* **352**, 1190–1194, DOI: [10.1126/science.aaf6644](https://doi.org/10.1126/science.aaf6644) (2016). <https://www.science.org/doi/pdf/10.1126/science.aaf6644>.
24. Arbabi, A. *et al.* Increasing efficiency of high numerical aperture metasurfaces using the grating averaging technique. *Sci. Rep.* **10**, 7124, DOI: [10.1038/s41598-020-64198-8](https://doi.org/10.1038/s41598-020-64198-8) (2020).
25. Shalaginov, M. Y. *et al.* Single-element diffraction-limited fisheye metalens. *Nano Lett.* **20**, 7429–7437, DOI: [10.1021/acs.nanolett.0c02783](https://doi.org/10.1021/acs.nanolett.0c02783) (2020). PMID: 32942862, <https://doi.org/10.1021/acs.nanolett.0c02783>.
26. Chung, H. & Miller, O. D. High-na achromatic metalenses by inverse design. *Opt. Express* **28**, 6945–6965, DOI: [10.1364/OE.385440](https://doi.org/10.1364/OE.385440) (2020).
27. Menon, R. Github page for this memorandum. [retrieved 22 Feb 2023], <https://github.com/RajeshMenonNano/OpticaMemo>.
28. Engelberg, J. & Levy, U. Standardizing flat lens characterization. *Nat. Photonics* **16**, 171–173 (2022).
29. Buralli, D. A. & Morris, G. M. Effects of diffraction efficiency on the modulation transfer function of diffractive lenses.

- Appl. Opt.* **31**, 4389–4396, DOI: [10.1364/AO.31.004389](https://doi.org/10.1364/AO.31.004389) (1992).
30. Khorasaninejad, M. *et al.* Polarization-insensitive metalenses at visible wavelengths. *Nano Lett.* **16**, 7229–7234, DOI: [10.1021/acs.nanolett.6b03626](https://doi.org/10.1021/acs.nanolett.6b03626) (2016). PMID: 27791380, <https://doi.org/10.1021/acs.nanolett.6b03626>.
 31. Xiao, X. *et al.* Large-scale achromatic flat lens by light frequency-domain coherence optimization. *Light. Sci. Appl.* **11** (2022).
 32. Park, J.-S. *et al.* All-glass, large metalens at visible wavelength using deep-ultraviolet projection lithography. *Nano Lett.* **19**, 8673–8682, DOI: [10.1021/acs.nanolett.9b03333](https://doi.org/10.1021/acs.nanolett.9b03333) (2019). PMID: 31726010.
 33. Mirotznik, M. S., Pustai, D. M., Prather, D. W. & Mait, J. N. Design of two-dimensional polarization-selective diffractive optical elements with form-birefringent microstructures. *Appl. Opt.* **43**, 5947–5954, DOI: [10.1364/AO.43.005947](https://doi.org/10.1364/AO.43.005947) (2004).
 34. Ford, J. E., Xu, F., Urquhart, K. & Fainman, Y. Polarization-selective computer-generated holograms. *Opt. Lett.* **18**, 456–458, DOI: [10.1364/OL.18.000456](https://doi.org/10.1364/OL.18.000456) (1993).
 35. Kim, G., Domínguez-Caballero, J. A. & Menon, R. Design and analysis of multi-wavelength diffractive optics. *Opt. Express* **20**, 2814–2823, DOI: [10.1364/OE.20.002814](https://doi.org/10.1364/OE.20.002814) (2012).
 36. Kim, G., Dominguez-Caballero, J. A., Lee, H., Friedman, D. J. & Menon, R. Increased photovoltaic power output via diffractive spectrum separation. *Phys. Rev. Lett.* **110**, 123901, DOI: [10.1103/PhysRevLett.110.123901](https://doi.org/10.1103/PhysRevLett.110.123901) (2013).
 37. Meem, M., Majumder, A. & Menon, R. Multi-plane, multi-band image projection via broadband diffractive optics. *Appl. Opt.* **59**, 38–44, DOI: [10.1364/AO.59.000038](https://doi.org/10.1364/AO.59.000038) (2020).
 38. Mohammad, N., Meem, M., Wan, X. & Menon, R. Full-color, large area, transmissive holograms enabled by multi-level diffractive optics. *Sci. Rep.* 5789, DOI: [10.1038/s41598-017-06229-5](https://doi.org/10.1038/s41598-017-06229-5) (2017).
 39. Magnusson, A., Moud, K. K. & Hård, S. A new, sensitive diffractive optic angle meter. In *Diffractive Optics and Micro-Optics*, DTuB2, DOI: [10.1364/DOMO.2002.DTuB2](https://doi.org/10.1364/DOMO.2002.DTuB2) (Optica Publishing Group, 2002).
 40. Wang, A. *Angle sensitive pixels for integrated light field sensing*. Ph.D. thesis, Cornell University (2012).

Acknowledgements

Support from grants #N6560-NV-ONR and NASA #NNL16AA05C are gratefully acknowledged. The authors thank H. Smith, H. Li and O. Miller for fruitful discussions.

Author contributions statement

All authors reviewed the manuscript.

Competing interests RM has financial interest in Oblate Optics, Inc., which is commercializing flat lenses.